Use of spatially refined satellite remote sensing fire detection data to initialize and evaluate coupled weather-wildfire growth model simulations

Janice L. Coen[1] and Wilfrid Schroeder[2]

Received 3 September 2013; revised 3 October 2013; accepted 5 October 2013.

[1] Large wildfires may grow for weeks or months from ignition until extinction. Simulating events with coupled numerical weather prediction (NWP)–wildland fire models is a challenge because NWP model errors grow with time. A new simulation paradigm was tested. Coupled Atmosphere-Wildland Fire Environment model simulations of the 2012 Little Bear Fire in New Mexico were implemented for multiple days of fire growth from ignition and then used spatially refined (375 m) 12 h satellite active fire data derived from the Visible Infrared Imaging Radiometer Suite (VIIRS) to initialize a fire in progress. The simulations represented fire growth well for 12–24 h after each initialization in comparison to later satellite passes but strayed from mapped area with time. A cycling approach, in which successive VIIRS perimeters were used to initialize fire location for the next 12 h period, overcame this and can be used with cycled weather forecasts to predict even a long-lived fire's lifecycle.
Citation: Coen, J. L., and W. Schroeder (2013), Use of spatially refined satellite remote sensing fire detection data to initialize and evaluate coupled weather-wildfire growth model simulations, *Geophys. Res. Lett.*, *40*, doi:10.1002/2013GL057868.

1. Introduction

[2] Large wildfires can cover hundreds of thousands of acres and continue for months, varying in intensity as they encounter different environmental conditions such as terrain, fuel properties and condition, and weather, which may vary dramatically in time and space during a single fire. Weather—primarily wind, but also humidity—can be the most important factor shaping fires (J. L. Coen and P. J. Riggan, Simulation and thermal imaging of the 2006 Esperanza Wildfire in Southern California: Application of a coupled weather-wildland fire model, submitted to *International Journal of Wildland Fire*, 2012) and, compared to fuels and terrain, is the most rapidly changing. Current kinematic operational fire behavior simulation tools, including FARSITE [*Finney*, 1998] and BehavePlus [*Andrews*, 2009], estimate the rate of spread of the leading edge of a wildfire—the operational criteria of most concern—using terrain slope, fuel properties and moisture state, and instantaneous (usually point) weather measurements. More recently, modeling systems that join a full numerical weather prediction (NWP) model with wildfire behavior components (i.e., coupled weather-wildfire models) have been developed [*Coen*, 2013; *Coen et al*., 2012] and applied to landscape-scale fires. In addition to modeling a fire's growth, they can represent the unique characteristics of each fire—the perimeter shape, bifurcation into multiple heading regions, and production of flank runs—and capture fire dynamic phenomena such as fire whirls, horizontal roll vortices, and blowups. In addition to being used retrospectively to study past fires, these models can be run in a predictive sense to anticipate the future extent and behavior of existing wildfires. They are applicable to a broad range of geophysical research, including biomass burning, regional air quality, and land surface impacts.

[3] Data for validation of or assimilation into such models (both meteorological and fire related) are limited. Surface weather station data are usually sparse due to the remoteness of many fires. Likewise, fire mapping and monitoring has been done piecemeal. The USDA Forest Service FireMapper airborne infrared mapping radiometer has provided unsaturated high-resolution mapping data on wildfires of opportunity and, in addition to the USDA Forest Service National Infrared Operations (NIROPs) nighttime airborne mapping, has been used as an intelligence resource for high-priority wildland fire operations. Infrared imaging sensors on polar orbiting and geostationary satellites typically produce subhourly to 12 hourly maps of active fires with nominal pixels varying between 1 and 4 km [*Giglio et al*., 2003; *Prins and Menzel*, 1992]. Satellite data have, for more than two decades, provided routine active fire information but have not been able to distinguish between individual fire lines or to validate fire behavior on all but the largest fires [*Loboda and Csiszar*, 2007]. Most significantly, modeling and monitoring have been done separately, with models simulating fires from their ignition or first report.

[4] Forecasting of wildfire growth using coupled weather-fire models relies on an accurate NWP forecast and authentic representation of fire behavior in response to environmental conditions, as well as the interactions between them. Thus, the issues that plague weather modeling extend to coupled weather-fire modeling as well. Notably, the skill of forecasts in simulating future states decreases with time, particularly for small-scale features [*Lorenz*, 1969; *Lilly*, 1990]. The consequences for coupled weather-fire model simulations of wildfires are threefold. First, during a long-lasting fire when an ignition initially grows slowly or a fire experiences a multiday lull in activity, a simulation initialized before ignition could lose most of its fidelity—in both weather and predicted fire location—before the time of active fire growth or period of interest due to error growth arising from imperfect initialization data and model physics. Second, wildfires may grow for weeks to months, but because weather forecast skill decreases with

[1]National Center for Atmospheric Research, Boulder, Colorado, USA.
[2]Department of Geographical Sciences, University of Maryland, College Park, Maryland, USA.

Corresponding author: J. L. Coen, National Center for Atmospheric Research, PO Box 3000, Boulder, CO 80307-3000, USA. (janicec@ucar.edu)

0094-8276/13/10.1002/2013GL057868

time, even synoptic-scale models essentially losing all skill after 12 days [*Dalcher and Kalnay*, 1987], no single weather forecast can cover a long-lived event accurately. Forecasting techniques such as cycling [*Benjamin et al*., 1991] have been developed to address this issue and exploit the periodic arrival of updated atmospheric state data. Third, even if the wildfire behavior module accurately parameterized physical processes and the coupled model showed high predictive skill, wildfires may produce long-distance spotting, in which burning embers are lofted ahead of the fire line, igniting additional fires. This process is not included because it is inherently stochastic and, although it may be treated in a probabilistic manner, is unsuitable for treatment by deterministic models; however, spotting can dramatically affect a fire's outcome where it occurs frequently [*Luke and McArthur*, 1978]. Similarly, fire suppression by ground or airborne crews can reshape the fire perimeter and spread rate, thereby requiring routine diagnostics and model reinitialization.

[5] We present results for a wildfire in June 2012 in New Mexico using an innovative approach to improve the simulation of large, long-duration wildfires, either for retrospective studies or forecasting in a number of geophysical applications. The approach utilizes spatially refined (375 m) satellite active fire data to initialize and evaluate fire growth model predictions.

2. Materials and Methods

2.1. Coupled Atmosphere-Wildland Fire Environment Model

[6] Coupled Atmosphere-Wildland Fire Environment (CAWFE) combines a NWP model [*Clark et al*., 1997] with a fire behavior module [*Coen*, 2005, 2013] that describes the propagation of a wildland fire in response to terrain, fuels, temporally evolving weather, and weather's impact on fuel moisture. Near-surface atmospheric winds are used to calculate the direction and spread rate of the fire, which releases sensible heat, latent heat, and smoke into the lower atmosphere at rates that vary in space and time according to the fuel consumption rate. The fire's heat fluxes, in turn, alter the atmospheric state, including winds directing the fire. Fire module components treat physical processes on two-dimensional fuel cells on the surface that are further refined from atmospheric three-dimensional grid cells. Processes include the flaming front's rate of spread, postfrontal heat release, crown fire ignition and consumption, and upscaling of heat fluxes to the atmospheric model. An additional algorithm defines the subgrid-scale interface between burning and unignited fuel as it passes through fuel cells. CAWFE does not explicitly simulate flames or combustion but parameterizes these subgrid-scale processes with semiempirical and empirical relationships.

[7] Prior simulations with dynamic models have modeled wildland fire evolution from ignition as either a point source or a line. In nature, fires ignited by lightning strikes may smolder for days or grow slowly at sizes or intensities too low for detection before erupting when more favorable dry and/or windy conditions occur. In addition to occurring at such small scales that NWP models have difficulty capturing boundary layer wind fluctuations, effects such as local fuel variations, which are unlikely to be known, dominate fire growth in weakly forced fires. Hence, large errors are likely. Instead, we introduce a fire perimeter defined by Visible Infrared Imaging Radiometer Suite (VIIRS) pixel-based fire detection data into a running NWP model at a time corresponding to the observation and allow the fire to evolve. At the time of the next VIIRS data (~12 h later), we compare the simulated and observed fire extent.

2.2. Satellite Remote Sensing Active Fire Detection Data

[8] The Visible Infrared Imager Radiometer Suite launched in October 2011 aboard the Suomi National Polar-orbiting Partnership (S-NPP/VIIRS) provides enhanced Earth monitoring capabilities compared to previous polar orbiting systems, achieving complete global coverage every 12 h or less at nominal spatial resolutions of 375 m and 750 m [*Justice et al*., 2013]. The new VIIRS 375 m active fire detection data applied in this study have been successfully used to detect both small prescribed fires as well as large wildfires in different geographic regions, with fire mapping skills verified by ground and aerial survey (I. Csiszar et al., Active fires from mid-wave measurements of the Suomi NPP Visible Infrared Imager Radiometer Suite: Product status and first evaluation results, submitted to *Journal of Geophysical Research*, 2013, http://www.nasa.gov/mission_pages/NPP/news/west-blazes.html). Compared to existing 1 km resolution polar orbiting sensor data, VIIRS 375 m fire data allow for improved—and often earlier—detection of smaller and/or cooler fires and spatially explicit delineation of large wildfire flaming fronts. Initial assessment of VIIRS 375 m fire algorithm performance using data acquired over small prescribed fires with temperatures around 650–1000 K indicated a minimum detectable fire size ranging from 0.004% (nighttime data) to 0.02% (daytime data) of the effective pixel area (unpublished data). Continuous acquisition of VIIRS global data and processing of active fire detections provided routine observations around 2:30 P.M. and 2:30 A.M. MDT in this study area. Smoke does not prevent the VIIRS fire detection, but fires occurring under optically thick clouds such as cumulus or under nonburning closed canopies (e.g., surface fires in tropical forests) are normally not detected.

2.3. Application to the 2012 Little Bear Fire

[9] The Little Bear Fire burned 17,939 ha (44,330 ac) and 254 buildings and was the most destructive in New Mexico state history. It was ignited at 1:00 P.M. MDT on 4 June 2012 in the Sierra Blanca Mountains of south central New Mexico by a lightning strike and stayed dormant during the initial 72 h. Favored by a gradual decrease in relative humidity and a rapid increase in wind gusts, the fire began to spread rapidly on 8 June, 1–2 h before the first VIIRS active fire detection at 20:31 UTC (2:31 P.M. MDT), creating an 18 km long complex only 24 h after first detection. The fire continued to burn for 3 weeks, progressing along the north and south flanks produced by the fast-moving flaming front initially traveling west to east.

[10] National Centers for Environmental Prediction (NCEP) Final Operational Global Analysis gridded atmospheric data were used for CAWFE initialization and later boundary conditions of four nested domains with horizontal grid resolutions of 10 km, 3.3 km, 1.1 km, and 370 m. The terrain in domain 4 is shown in Figure 1a. The spatial distribution of fuel models, categorized using *Anderson's* [1982] fuel classification system (Figure 1b), was obtained from LANDFIRE (http://www.landfire.gov) and resampled to model fuel cells (5 × 5 lay within the footprint of each atmospheric grid cell) using nearest-neighbor resampling. The fire encountered a mix of forest fuel types at higher elevations near the ignition location and mixed shrubs and grasses on lower elevation rangelands at later times. Fuel moisture of dead fine fuels was diagnosed

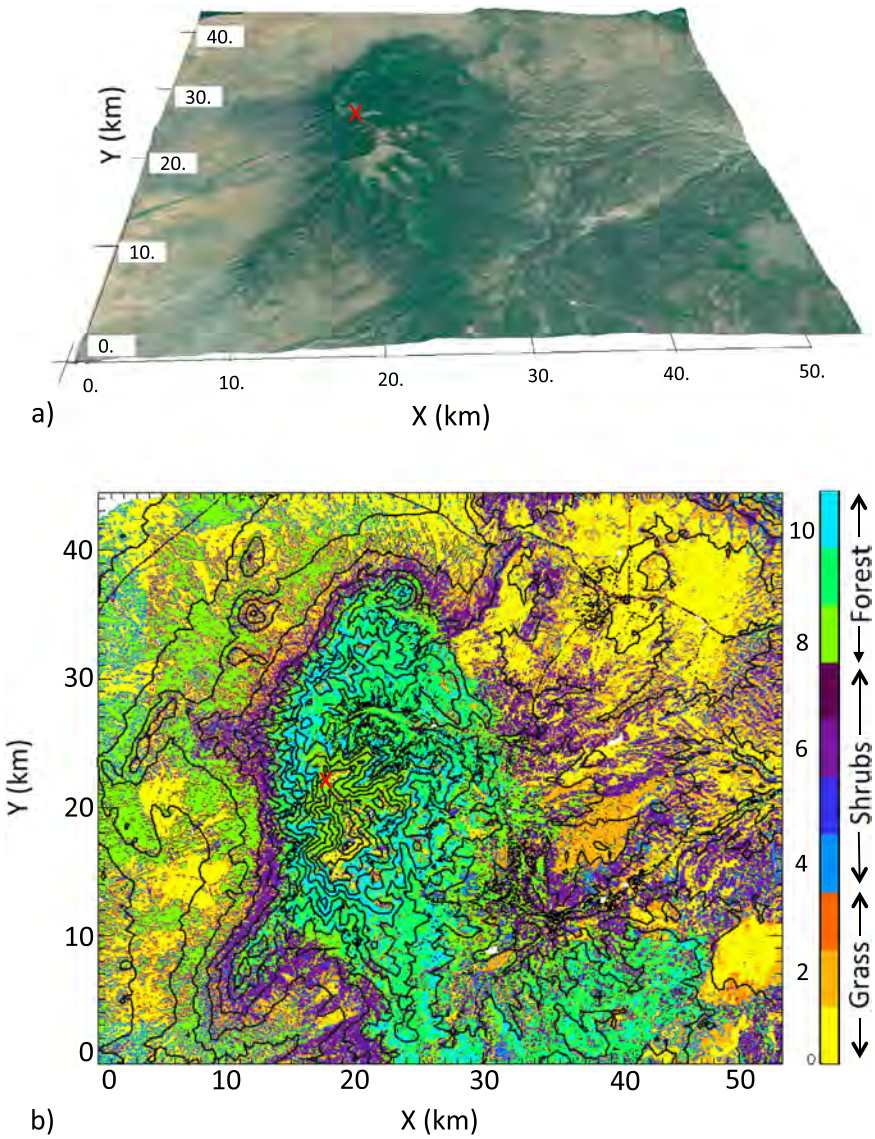

Figure 1. (a) Terrain in the innermost (fourth) domain. (b) Fuel models, with terrain contours every 150 m. The ignition location is shown with a red "X".

(J.Bishop, personal communication) from measured relative humidity at the Mescal Remote Automated Weather Station upwind of the fire.

[11] CAWFE was applied in two ways to the Little Bear Fire. First (EXPT0), CAWFE simulated the weather for 6 h preceding ignition and, after igniting a point at the time and location of the detected strike, continued to model the weather and fire growth for 4 days, at which time the fire extent was compared with that of the first VIIRS detection.

[12] Three other simulations used the same configuration initialized 4 days later on 8 June at 7 A.M. MDT, 7.5 h before the first fire detection. In each, the active fire line was first introduced, in progress, at the times of the first (EXPTA), the second (EXPTB), or the third (EXPTC) VIIRS overpass, respectively, using the outermost detected active fire pixels to define ignited fuel cells in the model. In each experiment, the coupled weather and fire growth was modeled until 10 June at 08:33 UTC (2:33 P.M. MDT); modeled fire dimensions were compared with the fire extent from subsequent passes.

3. Results

[13] First detection of the Little Bear Fire using VIIRS 375 m data occurred on 8 June at 2:31 P.M. MDT (Figure 2). The initial satellite-based fire perimeter was approximately 2 km in diameter, coinciding with a small fire pixel cluster located near the reported ignition point. The next VIIRS data on 9 June at 2:56 A.M. MDT showed a considerably larger fire-affected area extending approximately 14 km east from the ignition point and 5 km across. The following VIIRS observation on 9 June at 2:14 P.M. MDT showed that the fire had continued to grow albeit at a lower spread rate, extending eastward another 4 km. From this time on, the fire had bifurcated into two main heading regions extending along the northern and southern edges of the complex spreading perpendicular to its original eastward trajectory.

[14] EXPT0, the 4 day simulation of the fire from ignition, overpredicted the fire extent at the first VIIRS detection as an approximately 4 km versus a 2 km diameter circle

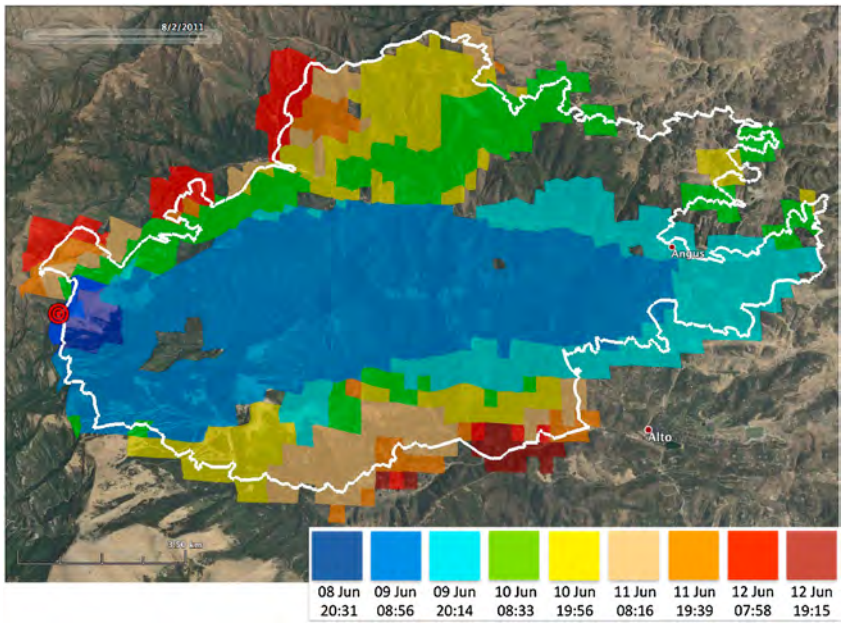

Figure 2. The first nine VIIRS active fire detection polygons during the Little Bear Fire and the perimeter mapped by USDA Forest Service NIROPs (white line) at 11:10 P.M. MDT on 11 June (12 June, 05:10 UTC). Colors indicate detected fire extent at different overpass dates and times (UTC) (see color bar).

(Figure 3), overestimating the area by a factor of 3. This error represented the accumulated effects of model errors in wind speed and humidity on fire growth—growth driven by afternoon gustiness and dry fuels and suppressed by higher atmospheric humidities that created fine fuel moistures that fluctuated near and, at night, above values at which fire could not spread. Model fidelity decreased by day 4; the model did not capture the growth just before the first VIIRS detection.

[15] As an alternative to continuing EXPT0 further into the active growth period with already substantial errors in fire extent and a 4 day old weather forecast, a new approach was used. EXPTA began with a recently initialized weather simulation into which the fire was first introduced as covering the area of the first detection and continued for 1.5 days. Compared to the next observation 12 h later (Figure 4), EXPTA captured the fire extent, reaching only 1.3 km farther to the south and 1.3 km shorter in downwind extent than VIIRS data showed; the simulation successfully captured the shape, direction of spread, and distinguishing features such as bifurcation around a river valley and rejoining.

[16] Figure 5 shows the modeled fire extent in EXPTA, EXPTB, and EXPTC, in which the perimeter was initialized at different times using the VIIRS-derived active fire detections and the simulations were run until 10 June at 08:33 UTC, the time of the fourth pass. Extending EXPTA throughout the fire's life was ineffective. During the next 24 h, EXPTA strayed further from the observed extent each 12 h of simulation time (Figures 5c and 5d), with erroneous growth from the north and south flanks. In contrast, simulation of this 12 h period with EXPTB, in which the fire was initialized with the second VIIRS fire map (Figure 5e), was superior, capturing the spread 8 km eastward (Figure 5f) and then to the northeast, although it produced 1.0–2.5 km of growth from the southern side of the fire through forest fuels that was not observed to occur, perhaps due to differences in the forest litter fuel properties at lower elevations from those given by the forest litter category. It then (Figure 5g) apparently overpredicted the growth of the fire's leading edge through grassy fuels on the plains by 5–7 km. EXPTC produced a similar growth during this period (Figure 5i). However, how range fuel patchiness affects fire spread is still an area of research [*McGranahan et al*., 2012], and the extensive fire suppression was not represented in the simulations. Burnouts could account for large increases in area but did not occur during this time (http://fam.nwcg.gov/famweb/hist_209/report_list_209). In addition, determining the precise extent of the burned area in the active fire detection map at this time (Figure 5j) was difficult, as the low intensities,

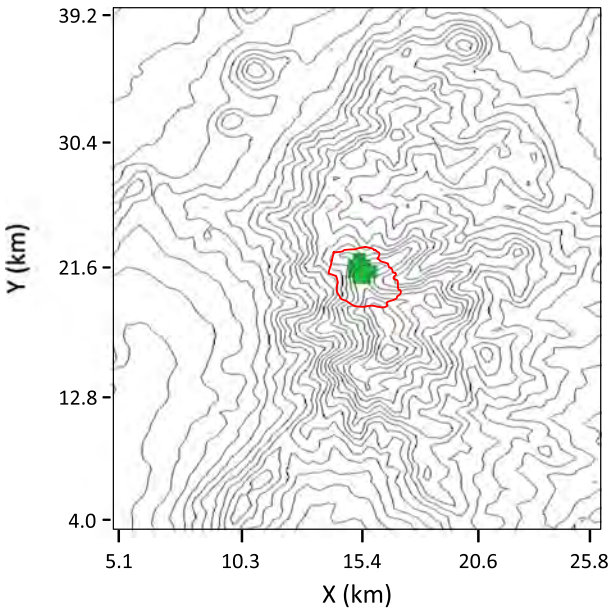

Figure 3. The extent of the simulated fire (red line) in EXPT0 at the time of the first VIIRS fire detection (green fill) on 8 June at 2:31 P.M. MDT. Terrain contours are shown every 88 m.

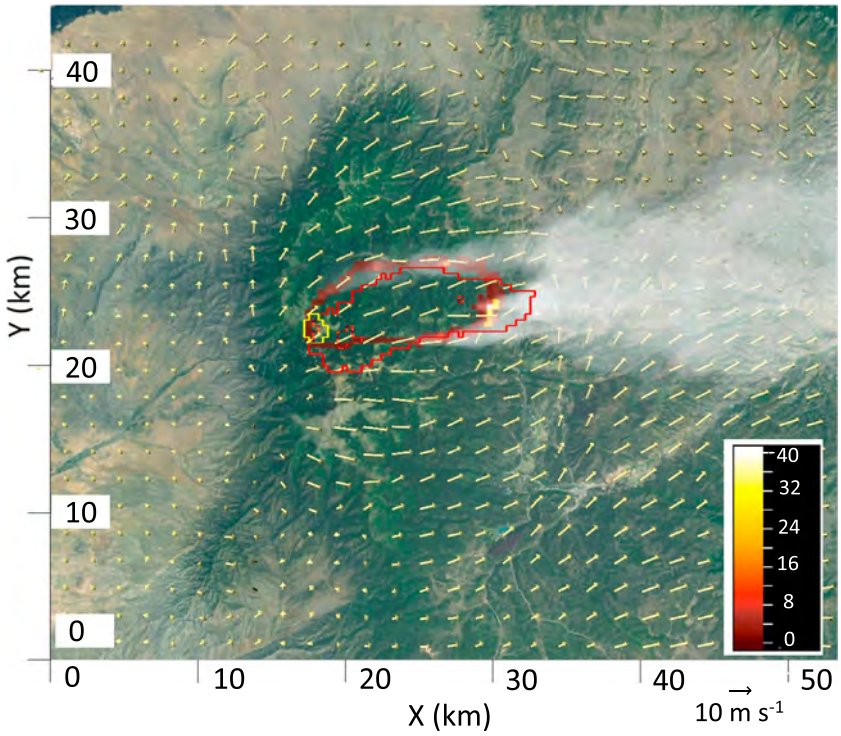

Figure 4. The VIIRS fire perimeter (yellow line) used for initializing fire location in EXPTA. The total heat flux (kW m^{-2}) (color bar) shows modeled fire extent 12 h later, along with coincident VIIRS data (red line), modeled winds at 21 m above-ground level, and modeled smoke mixing ratio (white).

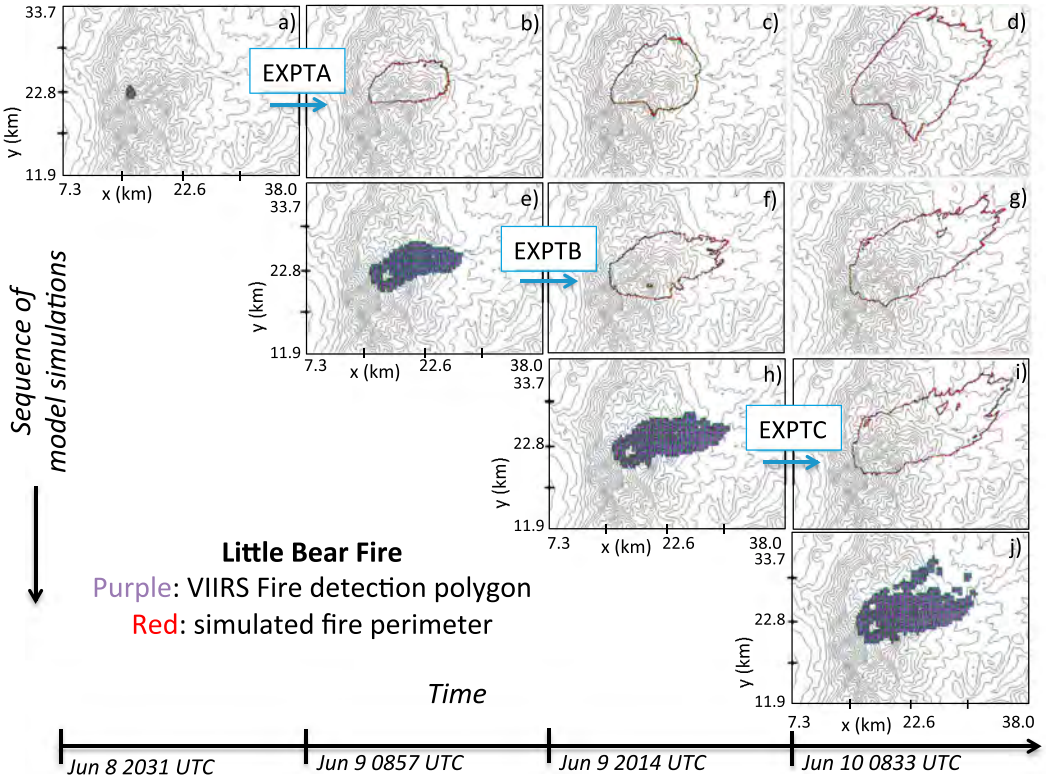

Figure 5. Modeled fire extent (red) in EXPTA, EXPTB, and EXPTC, in which the fire extent is initialized using the outermost VIIRS-derived active fire detection pixel. Active fire and burned interior pixels, mapped to model fuel cells, are indicated (purple fill). Each simulation is run until 10 June at 08:33 UTC, the time of the fourth pass. Terrain contours are plotted every 88 m. Black-rimmed frames indicate simulation sequences that, together, make up a cycling approach for modeling a wildfire's lifetime.

rapid fuel consumption, and rapid cooling of soils in patchy, low-load desert fuels made detection more challenging. In each successive experiment, initializing the fire with the newest detected extent allowed the simulation to remain largely on track for the next 12–24 h. Taken as a whole, Figure 5 demonstrates how a cycling approach, using sequential simulations for simulating successive periods of time, can model the lifetime of even a long-lived wildfire.

4. Discussion and Conclusions

[17] The high societal impact of wildfires calls for simulation tools for improved scientific understanding and prediction for decision support in wildfire response, air quality, and land surface impacts. These require high-fidelity simulations of weather, fire behavior, and their interactions throughout a wildfire's lifetime. While error growth arising from the nonlinear nature of weather models and fire dynamics limits how well a model performs, we have introduced an approach using new, routine spaceborne observations to overcome previous obstacles and allow simulation of wildfires and their impacts throughout their lifetimes. This work showed that simulating the fire from ignition could lead to accumulated errors from the model's deteriorating skill even before first detection and any detectable fire growth. Other simulations begun shortly before first detection, in which the fire was ignited in progress at the indicated times and using perimeters specified by satellite active fire detection data, showed the general features and extent of fire growth over each 12–24 h period with markedly reduced departures. Improvement from this approach arises from initialization with more current weather analyses and updated maps of fire location. Complementary higher-resolution but less frequent data from NIROPs, FireMapper, or Landsat-class spaceborne sensors are other potential inputs. The approach's significance is that configured as a forecast rather than a retrospective study, it can be applied using operational cycled weather forecasts such as NCEP's Rapid Refresh and High-Resolution Rapid Refresh as initialization data to predict a fire's growth from first detection until containment—a previously unattainable goal due to accumulation of model errors.

[18] **Acknowledgments.** This work was supported by the National Aeronautics and Space Administration under awards NNX12AQ87G and NNH11AS03, the National Science Foundation (NSF) under grant 0835598, and the Federal Emergency Management Agency under award EMW-2011-FP-01124. The National Center for Atmospheric Research is sponsored by NSF. Any opinions, findings, and conclusions or recommendations expressed in this material are the authors' and do not reflect the views of NSF.

[19] The Editor thanks two anonymous reviewers for their assistance in evaluating this paper.

References

Anderson, H. E. (1982), Aids to determining fuel models for estimating fire behavior, Intermountain Forest and Range Experiment Station General Technical Report INT-122, USDA Forest Service, Ogden, UT.

Andrews, P. L. (2009), BehavePlus fire modeling system, version 5.0: Variables, Rocky Mountain Research Station General Technical Report RMRS-GTR-213WWW Revised, USDA For. Serv., Fort Collins, Colo.

Benjamin, S. G., K. A. Brewster, R. L. Brummer, B. F. Jewett, T. W. Schlatter, T. L. Smith, and P. A. Stamus (1991), An isentropic three-hourly data assimilation system using ACARS aircraft observations, *Mon. Weather Rev.*, *119*, 888–906.

Clark, T. L., T. Keller, J. Coen, P. Neilley, H. Hsu, and W. D. Hall (1997), Terrain-induced turbulence over Lantau Island: 7 June 1994 Tropical Storm Russ case study, *J. Atmos. Sci.*, *54*, 1795–1814.

Coen, J. L. (2005), Simulation of the Big Elk Fire using coupled atmosphere-fire modeling, *Int. J. Wildland Fire*, *14*, 49–59.

Coen, J. L. (2013), Modeling wildland fires: A description of the Coupled Atmosphere-Wildland Fire Environment model (CAWFE), NCAR Tech. Note NCAR/TN-500+STR, Natl. Cent. for Atmos. Res., Boulder, Colo., doi:10.5065/D6K64G2G.

Coen, J. L., M. Cameron, J. Michalakes, E. G. Patton, P. J. Riggan, and K. M. Yedinak (2012), WRF-Fire: Coupled Weather-Wildland Fire Modeling with the Weather Research and Forecasting Model, *J. Appl. Meteorol. Climatol.*, *52*, 16–38.

Dalcher, A., and E. Kalnay (1987), Error growth and predictability in operational ECMWF forecasts, *Tellus*, *39*, 474–491.

Finney, M. A. (1998), FARSITE: Fire Area Simulator—Model development and evaluation, Rocky Mountain Station, Research Paper RMRS-RP-4, 47 pp., USDA For. Serv., Fort Collins, Colo.

Giglio, L., J. Descloiters, C. O. Justice, and Y. Kaufman (2003), An enhanced contextual fire detection algorithm for MODIS, *Remote Sens. Environ.*, *87*, 273–282.

Justice, C. O., et al. (2013), Land and cryosphere products from Suomi NPP VIIRS: Overview and status, *J. Geophys. Res. Atmos.*, *118*, 9753–9765, doi:10.1002/jgrd.50771.

Lilly, D. K. (1990), Numerical prediction of thunderstorms—Has its time come?, *Q. J. R. Meteorol. Soc.*, *116*, 779–798.

Loboda, T., and I. Csiszar (2007), Reconstruction of fire spread within wildfire fire events in Northern Eurasia from the MODIS active fire product, *Global Planet. Change*, *56*(3–4), 258–273.

Lorenz, E. N. (1969), The predictability of a flow which possesses many scales of motion, *Tellus*, *21*, 289–307.

Luke, R. H., and A. G. McArthur (1978), *Bushfires in Australia*, 359 pp., Aust. Gov. Serv., Canberra.

McGranahan, D. A., D. M. Engle, J. R. Miller, and D. M. Debinski (2012), An invasive grass increases live fuel proportion and reduces fire spread in a simulated grassland, *Ecosystems*, *16*, 158–169.

Prins, E. M., and W. P. Menzel (1992), Geostationary satellite detection of biomass burning in South America, *Int. J. Remote Sens.*, *13*, 2783–2799.